ACS OMEGA

http://pubs.acs.org/journal/acsodf

Article

The Shape of Heavy Droplets on Superhydrophobic Surfaces

Yang Yu,* Cunjing Lv, Lifeng Wang, and Peiliu Li

Cite This: *ACS Omega* 2020, 5, 26732−26737

Read Online

ACCESS | Metrics & More | Article Recommendations

ABSTRACT: An analytical model is developed to describe the shape of heavy droplets on solid surfaces with arbitrary wetting properties (corresponding to the contact angles ranging from 0 to 180°). This model, based on a surface of revolution by rotating two elliptic arcs, reduces to the ellipsoid model for a hydrophilic case. Experimental measurements are also conducted to verify the model. It shows that the mean curvature distribution of the developed model agrees well with that of real droplets on hydrophobic surfaces, even on superhydrophobic surfaces. For water droplets with a volume up to 1000 μL on superhydrophobic surfaces having a 162° contact angle, the errors of the predicted heights, maximum radius, and wetting radius using this model are less than 1.7%, which suggests the capability of this model in studying the wettability of heavy droplets. This model provides an accurate theoretical basis for designing and controlling the spread, transport, condensation, and evaporation of heavy droplets on superhydrophobic surfaces.

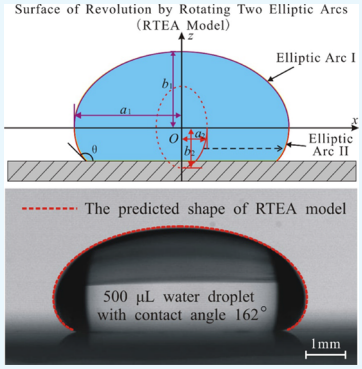

1. INTRODUCTION

Spread, transport, condensation, and evaporation of droplets have important applications in many fields,[1−6] such as microfluidic, micro-electromechanical systems (MEMS), medical apparatus and instruments, chemical engineering, and biological engineering. In these processes, both the droplet shape and wetting property of solid surfaces affect the dynamic behaviors of the system. The height, maximum cross section, and wetting area of the droplet, which are determined by its shape, have key effects on the driving forces and resistance forces. Superhydrophobic surfaces[7−9] with high contact angles ($\theta > 150°$) and very low rolling angles ($\alpha < 5°$) can help droplets to move and transport more freely and faster. In nature, raindrops can run down from the lotus leaves[10] and rice leaves[11] very easily due to the superhydrophobicity of leaves. In daily life, droplets moving and transporting on solid surfaces have a wide range of applications in clinical diagnostic screening,[12,13] condenser systems,[14] and biomedical applications.[15]

The equilibrium shape of a droplet is determined by the Young−Laplace equation,[16] $2\gamma H = \Delta p$, where γ is the surface tension, H is the mean curvature, and Δp is the Laplace pressure. The challenge lies in the fact that the Young−Laplace equation cannot be solved analytically except in a few special cases;[17,18] therefore, a lot of efforts have been made to solve it numerically. An alternative approach is to approximate the shape of the droplet with an a priori assumed profile. Approximate curved surfaces are widely used to replace the real shape of droplets to analyze or study the corresponding dynamic and static behaviors.[19−21] Generally, the effect of gravity could be neglected when the characteristic scale of the droplet is much smaller than the capillary length $l_c = \sqrt{\gamma/\rho g}$, where ρ is the mass density of the liquid and g is the gravitational acceleration. In this case, the Laplace pressure Δp is almost a constant and the spherical cap model can well describe the shape of the droplets,[8] and the variable radius cap model is used for the droplets on a cylinder surface.[22] The superhydrophobic surfaces are always rough. Unlike smooth, homogeneous, and uncontaminated surfaces where the solid−liquid−vapor three-phase contact line of the droplet is circular, microdecorated surfaces offer anisotropic energy barriers such that the depinning contact angles vary along the perimeter and the contact line shape is polygonal.[23] The rotational symmetry model cannot correctly predict such contact lines. However, the energy barriers could decrease to very low values and become identical when the size and space of the microstructure are small.[24] Under such scenarios, the three-phase contact line of the droplet is almost circular on these superhydrophobic surfaces, and the rotational models are available.

However, the effects of gravity should be considered when the characteristic scale of the droplet is larger than the capillary length. Gravity affects the shape of droplets and also the dynamic behavior of droplets, such as dynamic advancing angle, receding angle, and sliding angle.[25] There are a lot of practical applications related to heavy droplets, ranging from liquid marbles,[26] long-distance liquid transport behaviors,[27] liquid lenses,[28,29] to medical liquid samples.[12] In this regard, a

Received: August 3, 2020
Accepted: September 22, 2020
Published: October 7, 2020

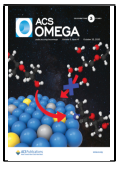

https://dx.doi.org/10.1021/acsomega.0c03700
ACS Omega 2020, 5, 26732−26737

new and more convenient method that could capture the geometry properties of heavy droplets is necessary and highly desired. For heavy droplets, the Laplace pressure Δp of the whole droplet is not a constant but a linear distribution along the gravity direction. Previously, the oblate spheroid model[30] and ellipsoid model[31,32] were widely used to approximately describe the shape of heavy droplets instead of the spherical cap model. The oblate spheroid model was proposed depending on minimization of the total energy, and this model could be used to calculate the shape and contact angle of heavy droplets.[30] The ellipsoid model was built by assuming that the droplet takes the shape of an oblate spheroidal cap and by minimizing the corresponding free energy, and it was verified that this model is accurate for the contact angle below about 120° and the size on the order of the capillary length.[31] Another ellipsoid model based on the volume and contact angle was proposed for investigating heavy droplets on flat and spherical solid surfaces.[32] It showed that the droplet height and wetting radius given by the ellipsoid model well fitted the results of Surface Evolver simulations under the conditions that the volume was less than 100 μL and the contact angle was less than 120°. The ellipsoid model was also used to study the evaporation of sessile drops (0.3−1.5 mm) on polymer surfaces and fitted the experimental data better than using the spherical model.[33] Furthermore, the ellipsoid model was also employed to study the shape of droplets and to calculate the contact angles on anisotropic surfaces.[34]

Even though, on hydrophilic surfaces (θ < 90°), these ellipsoid models are in good agreement with the shape of heavy droplets for droplet sizes on the order of the capillary length, they are not able to give a very good description of the heavy droplet shape on surfaces with moderate hydrophobicity (90° < θ < 120°). Moreover, all of them cannot describe the shapes of heavy droplets on superhydrophobic surfaces due to symmetric problems. In these models, the upper part of the droplet is simply assumed to be symmetric to its lower counterpart, which is inconsistent with the Young−Laplace equation. Consequently, there is no physically correct solution. In this work, we develop an analytical model to describe the shape of heavy droplets on flat solid surfaces with arbitrary wetting properties (corresponding to the contact angles ranging from 0 to 180°). The model is based on a surface of revolution by rotating two elliptic arcs (RTEA). For water droplets with a volume up to 1000 μL on superhydrophobic surfaces, the proposed model can accurately predict the heights, maximum radius, and wetting radius. The model developed in this paper is promising to analyze and understand the natural wetting states of large droplets, shedding new light on optimizing solid surfaces to control their capillary behaviors.

2. THEORY AND METHOD

The equilibrium shape of a droplet on a flat solid surface is a surface of revolution with a central axis. The Cartesian coordinate system is established as shown in Figure 1. The x axis is along the maximum radius and parallel to the solid surface. The z axis is along the central axis, and the y axis is perpendicular to both the x axis and z axis. The shape of the droplet on hydrophilic surfaces is entirely only one part, and it is the same as the ellipsoid model, whereas it is considered to be composed of two parts (Part I as the black line and Part II as the red line) that are divided by the xOy plane on hydrophobic surfaces. These two parts are both surfaces of

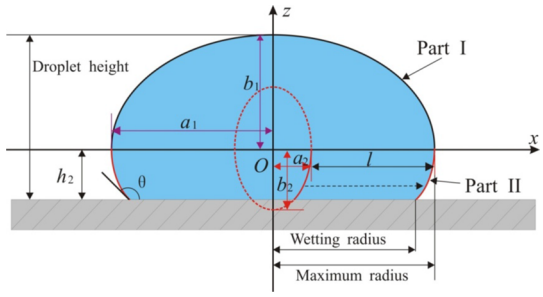

Figure 1. Schematic showing the theoretical model employed to approximately describe the shape of a heavy droplet. The coordinate system is established, and the geometrical parameters are indicated.

revolution that are obtained by two elliptic arcs rotating around the central axis. The semimajor axis and semiminor axis of the upper elliptic arc are a_1 and b_1 ($a_1 > b_1$), respectively. Those of the lower elliptic arc (as indicated by the red dashed line) are b_2 and a_2 ($b_2 > a_2$), respectively, and the lower arc needs a horizontal translation of distance l to keep the whole profile continuous.

The upper and lower surfaces of revolution are, respectively,

$$\frac{x^2}{a_1^2} + \frac{y^2}{a_1^2} + \frac{z^2}{b_1^2} = 1, \quad (z > 0) \tag{1}$$

$$\frac{(\sqrt{x^2 + y^2} - l)^2}{a_2^2} + \frac{z^2}{b_2^2} = 1, \quad (-h_2 < z < 0) \tag{2}$$

where h_2 is the height of the lower part, and the horizontal translation is

$$l = a_1 - a_2 \tag{3}$$

The translation leads to a continuous link of the upper part and lower part; meanwhile, the first derivative is also continuous automatically because the tangent lines of the joint of the two parts are both perpendicular to the x axis in the xOz cross section.

The mean curvature (H) is an average of the two principal curvatures (k_1 and k_2), i.e., $2H = k_1 + k_2$. The principal curvatures are the same at the same height due to rotational symmetry. The principal curvatures at every point of the elliptic arc in the xOz plane ($y = 0$) can represent the principal curvatures at the same height. Therefore, for the upper surface, the two principal curvatures are, respectively,

$$k_{1up} = \frac{a_1 b_1^4}{(a_1^2 z^2 - b_1^2 z^2 + b_1^4)^{3/2}} \tag{4}$$

$$k_{2up} = \frac{b_1^2}{a_1\sqrt{a_1^2 z^2 - b_1^2 z^2 + b_1^4}} \tag{5}$$

For the lower surface, they are

$$k_{1low} = \frac{a_2 b_2^4}{(a_2^2 z^2 - b_2^2 z^2 + b_2^4)^{3/2}} \tag{6}$$

$$k_{2low} = \frac{b_2^2\sqrt{b_2^2 - z^2}}{(a_2\sqrt{b_2^2 - z^2} + b_2 l)\sqrt{a_2^2 z^2 - b_2^2 z^2 + b_2^4}} \tag{7}$$

For each part, the difference in the Laplace pressure between the top point and the bottom point equals that generated by

https://dx.doi.org/10.1021/acsomega.0c03700
ACS Omega 2020, 5, 26732−26737

gravity (i.e., $\Delta p|_{z=0} - \Delta p|_{z=b1} = \rho g b_1$ and $\Delta p|_{z=-b2} - \Delta p|_{z=0} = \rho g b_2$, respectively), so we get

$$\gamma\left(\frac{a_1}{b_1^2} + \frac{1}{a_1}\right) - 2\gamma\frac{b_1}{a_1^2} = \rho g b_1 \tag{8}$$

$$\gamma\frac{b_2}{a_2^2} - \gamma\left(\frac{a_2}{b_2^2} + \frac{1}{a_2 + l}\right) = \rho g b_2 \tag{9}$$

In order to keep the pressure distribution (depending on the mean curvature of the interface) continuous across the combining site, the mean curvatures of these two parts are satisfied as

$$\frac{a_1}{b_1^2} + \frac{1}{a_1} = \frac{a_2}{b_2^2} + \frac{1}{a_2 + l} \tag{10}$$

It also keeps the second derivative of the model, which is related to the mean curvature continuous.

The volume of the droplet (V_0) and wetting property of the solid surface (contact angle θ) are known to provide the boundary conditions for the model. For the lower part (Part II), the elliptic arc will be cut by the solid surface at the tilt angle equal to the contact angle θ as illustrated in Figure 1. The slope is

$$\left.\frac{\partial z}{\partial x}\right|_{y=0,z=-h_2} = \tan(\pi - \theta) \tag{11}$$

where

$$h_2 = \frac{b_2^2}{\sqrt{(a_2\tan\theta)^2 + b_2^2}} \tag{12}$$

The droplet volume is the sum of the volumes of the two parts

$$V_0 = V_{\mathrm{PartI}} + V_{\mathrm{PartII}} = \frac{2}{3}\pi a_1^2 b_1 + \int_{-h_2}^{0} \pi x^2 \mathrm{d}z \tag{13}$$

The key parameters a_1, b_1, a_2, b_2, and l can be obtained by eqs 1−3 and eqs 8−13 for the given V_0 and θ. Then the shape of the heavy droplet can be described by the combined surfaces of revolution corresponding to eqs 1 and 2. The height (h), maximum radius (R_M), and wetting radius (R_W) of the heavy droplet are, respectively,

$$h = b_1 + h_2 \tag{14}$$

$$R_M = a_1 \tag{15}$$

$$R_W = \frac{a_2^2\tan(\pi - \theta)}{\sqrt{(a_2\tan\theta)^2 + b_2^2}} + l \tag{16}$$

3. RESULT AND DISCUSSION

The RTEA model developed here will reduce to the ellipsoid model for the hydrophilic case because the lower part is not included. The accuracy of the ellipsoid model had been discussed and verified by Lubarda and Talke[31] and Wang and Yu.[32] Besides the same ability as the ellipsoid model on hydrophilic surfaces, the main advantage of the RTEA model is for hydrophobic cases, especially for superhydrophobic cases. The nondimensional Bond number, Bo = $\rho g R_0/\gamma$, where R_0 is the characteristic scale of the droplet, is generally employed to represent the effect of gravity relative to the surface tension. The Bond number can also be expressed as Bo = $(R_0/l_c)^2$ associated with the capillary length l_c. If Bo ≪ 1, the effect of gravity on the shape can be neglected. If Bo > 1 corresponding to $R_0 > l_c$, the effect of gravity on the droplet shape must be considered and the RTEA model will be employed.

Two times value of the mean curvature (2 M. C.) and the two principal curvatures (P. C. 1 and P. C. 2) of the solution of the Young−Laplace equation, RTEA model, and ellipsoid model[32] are shown in Figure 2A, with volume V_0 = 500 μL

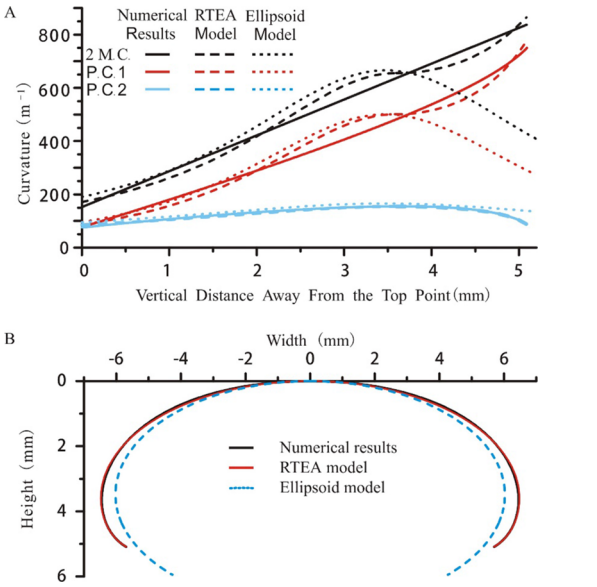

Figure 2. (A) Variation of the two times value of the mean curvature (2 M. C.), the principal curvature 1 (P. C. 1), and principle curvature 2 (P. C. 2) with the vertical distance away from the top point. The solid line, dashed line, and dot line represent the results of the numerical solution of the Young−Laplace equation, the RTEA model, and the ellipsoid model, respectively, for a 500 μL water droplet on a solid surface with a contact angle of 150°. (B) The droplet shape of the Young−Laplace equation solution and predicted shapes of the RTEA model and ellipsoid model.

(corresponding to Bo = 3.27) and contact angle θ = 150°. The principal curvature 1 is the curvature of the elliptic arc, and the principal curvature 2 is the curvature that is orthogonal to this elliptic arc. The mean curvature of the real droplet increases linearly along the opposite direction of the z axis. It shows that this increase is mainly from the increase of the principal curvature 1 (red solid line) and the principal curvature 2 increases slowly at first and then decreases (blue solid line). The mean curvature of the RTEA model keeps increasing continuously from Part I to Part II along the direction of gravity. It agrees with the mean curvature of the real droplet for the whole vertical distance, and the deviation is mainly from the principal curvature 1. So, the RTEA model (red solid line) is almost coincident with the real droplet shape (black solid line) shown in Figure 2B. For the ellipsoid model, the mean curvature does not always increase and will decrease below the maximum radius plane due to the symmetry. The main reason comes from the principal curvature 1. For describing the shape of the droplet on hydrophobic surfaces, the main errors of the ellipsoid model are caused by this decreasing stage of the mean curvature. A smaller mean curvature makes the shape shrink more slowly so that the same difference in the tilt angle from

https://dx.doi.org/10.1021/acsomega.0c03700
ACS Omega 2020, 5, 26732−26737

the maximum radius plane (the tilt angle 90°) to the contact plane with the solid surface (the tilt angle 180° − θ) needs a longer vertical distance. So, the droplet height in the ellipsoid model will be larger than the real height. Due to the volume conservation condition, it could be imagined that the maximum radius and wetting radius will be smaller than those of the real droplet. The comparison of the shapes of the real droplet (black solid line) and ellipsoid model (blue dashed line) clearly shows the difference in Figure 2B. However, the mean curvature does not deviate very much if the solid surface has moderate hydrophobicity, such as when the contact angle is in the range of 90° < θ < 120°. This is the reason why the ellipsoid model can describe the shape of heavy droplets on hydrophilic and moderate hydrophobic surfaces (i.e., θ < 120°).

Figure 3A shows the experimental results of the water droplet shapes with different volumes (V = 300 (Bo = 2.32), 500 (Bo = 3.27), 700 (Bo = 4.09), and 1000 μL (Bo = 5.18)) on the aforementioned superhydrophobic surface. The shapes are consistent with the solutions of the Young−Laplace equation (yellow solid line). It is verified again that the equilibrium shape of a droplet is determined by the Young−Laplace equation. The predicted surfaces by the RTEA model (red dashed line) fit the real droplet shapes very well even though the volume reaches 1000 μL. Moreover, compared with the real volume, the errors of the volume from the RTEA model are all less than 0.1%.

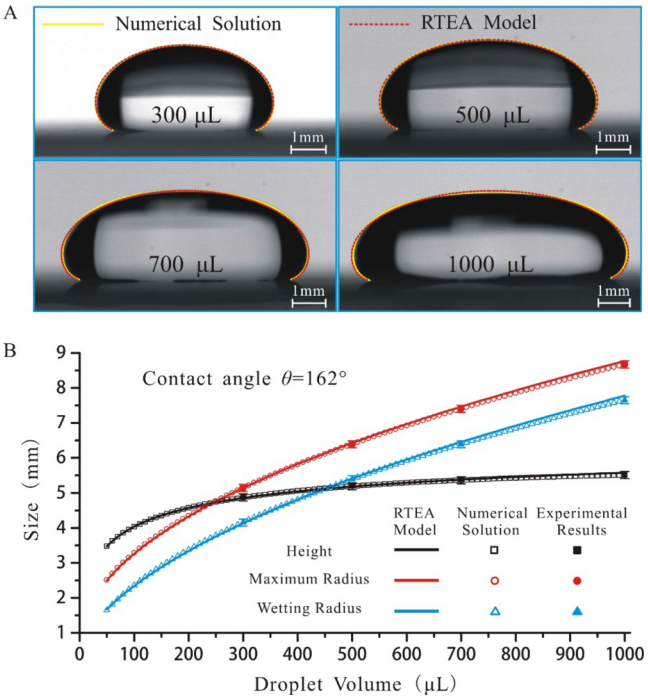

Figure 3. Comparisons of the predicted shapes by the RTEA model, numerical solutions, and real heavy droplets with different droplet volumes. (A) Experimental results of sessile water droplets with different volumes (300, 500, 700, and 1000 μL) on a superhydrophobic surface (θ = 162 ± 3°), numerical solutions as the yellow solid line, and predicted shapes by the RTEA model as the red dashed line. (B) The three key parameters varying with different volumes on a superhydrophobic surface (θ = 162°).

The key parameters of the droplet shape including height, maximum radius, and wetting radius are chosen to analyze the errors of the RTEA model. They are shown in Figure 3B with the volume of water droplets changing from 50 to 1000 μL on the fabricated superhydrophobic surface (θ = 162 ± 3°). It shows that all the errors of these parameters are very small (less than 1.7%) in this range of volumes. If the volume continues to increase, the droplet shape of the upper part will become more oblate and deviate from a half-ellipsoidal shape. The predicted maximum radius by the RTEA model will be larger. Figure 3B also suggests that the height of the water droplets increases slowly after the volume reaches a few hundreds of microliters. The height only changes 6.2% (from 5.19 to 5.51 mm) when the volume changes from 500 to 1000 μL. After this stage, the increased volume mainly compensates the increase of the maximum radius and wetting radius, and the height increases insignificantly.

To examine the ability of the RTEA model in different wetting properties, the comparison between the RTEA model (red solid line) and Young−Laplace solution (black dashed line) is further shown in Figure 4A. In this case, 500 μL volume water droplets with contact angles θ = 120, 150, and 180° are used, and the profiles of the droplet are obtained using numerical solutions of the Young−Laplace equation. It indicates that the predicted shapes are in very good agreement with the numerical profiles even if the contact angle reaches 180°.

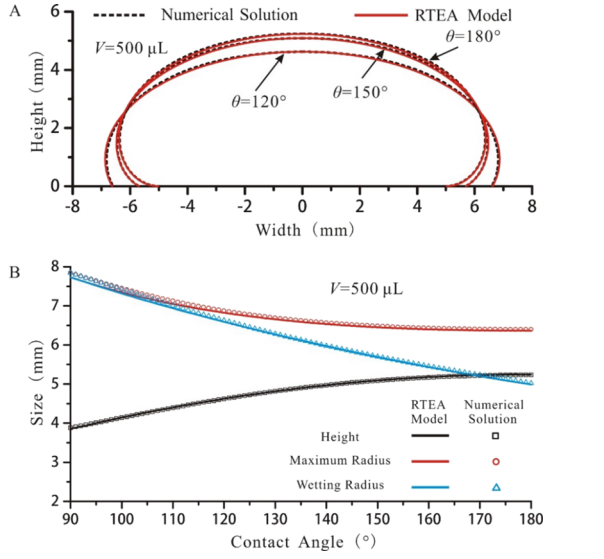

Figure 4. Comparisons of the predicted shapes by the RTEA model and numerical solutions with different contact angles. (A) Comparisons of the RTEA model and the Young−Laplace solution with a constant volume (V = 500 μL) on solid surfaces having different contact angles (θ = 120, 150, and 180°). (B) Variation of the three key parameters with the contact angle in the hydrophobic range.

Figure 4B shows the influence of these key parameters on a 500 μL water droplet on hydrophobic surfaces with different wetting properties (90° < θ < 180°). Both the maximum radius and the wetting radius decrease with increasing contact angle. However, the maximum radius decreases more slowly than the wetting radius. The height increases smoothly with contact angles. All the errors are lower than 1.5% in the whole hydrophobic regime. It also indicates that the RTEA model can describe the shape of a droplet on surfaces with higher contact angles (θ > 120°) even better than that with moderate hydrophobicity (90° < θ < 120°).

https://dx.doi.org/10.1021/acsomega.0c03700
ACS Omega 2020, 5, 26732−26737

4. CONCLUSIONS

The shape of heavy droplets deviates from a spherical cap and becomes an oblate spheroidal cap. The ellipsoid model can well describe the shape of heavy droplets with the size on the order of the capillary length on hydrophilic surfaces. By analyses of the mean curvature of the ellipsoid model on hydrophobic surfaces, it first keeps increasing to the plane with the maximum radius and then decreases to the contact plane with a solid surface. Considering that this distribution does not agree with the real case, the ellipsoid model cannot well predict the shape of heavy droplets on hydrophobic surfaces, especially on superhydrophobic surfaces. For droplets on hydrophobic and superhydrophobic surfaces, the mean curvature in the RTEA model could monotonously increase across the combined plane. Moreover, the RTEA model will have no lower part and be reduced to the ellipsoid model in hydrophilic conditions. Therefore, the RTEA model can describe the shape of heavy droplets with the size on the order of the capillary length on surfaces having arbitrary wettability ($0° < \theta < 180°$). In this range, the predicted height, maximum radius, and wetting radius of the RTEA model agree well with those of real droplets, and the errors are all less than 1.7%. The RTEA model could provide an accurate theoretical basis for designing and controlling the spread and transport of heavy droplets on superhydrophobic surfaces.

5. EXPERIMENTAL SECTION

Superhydrophobic glass slides were produced by treatment with a commercial coating agent (Glaco Mirror Coat Zero, Soft99, Co.) containing nanoparticles and an organic reagent.[35,36] The superhydrophobic coating was applied on the glass by pouring the Glaco liquid over the substrate. A thin liquid film wets the glass and dries in less than 1 min. The coated glass was then put into an oven and kept at 200 °C for 30 min. The pouring and heating processes were performed three times. After that, a contact angle $\theta = 162 \pm 3°$ was achieved. The contact angle and the shape of the droplet were measured using an OCA20 Device from DataPhysics (Germany). The droplet used in the measurement was made of deionized water.

AUTHOR INFORMATION

Corresponding Author

Yang Yu − *Department of Mechanics, School of Aerospace Engineering, Beijing Institute of Technology, Beijing 100081, China; Department of Mechanical Engineering, State University of New York at Stony Brook, Stony Brook, New York 11794, United States;* orcid.org/0000-0001-8092-2379; Email: yuyang08@bit.edu.cn

Authors

Cunjing Lv − *Department of Engineering Mechanics, School of Aerospace Engineering, Tsinghua University, Beijing 100084, China*

Lifeng Wang − *Department of Mechanical Engineering, State University of New York at Stony Brook, Stony Brook, New York 11794, United States;* orcid.org/0000-0002-2068-5102

Peiliu Li − *Department of Mechanics, School of Aerospace Engineering, Beijing Institute of Technology, Beijing 100081, China*

Complete contact information is available at: https://pubs.acs.org/10.1021/acsomega.0c03700

Notes

The authors declare no competing financial interest.

ACKNOWLEDGMENTS

This work was supported by the National Natural Science Foundation of China (Grant Nos. 11772052, 11632009, 11872227), China Scholarship Council (Grant No. 201706035002), and Tsinghua University (Grant No. 53330100318).

REFERENCES

(1) Zheng, Q. S.; Lv, C. J.; Hao, P. F.; Sheridan, J. Small is beautiful, and dry. *Sci. China Phys. Mech. Astron.* **2010**, *53*, 2245−2259.

(2) Wang, Y.; Zhao, Y.-P. Electrowetting on curved surfaces. *Soft Matter* **2012**, *8*, 2599−2606.

(3) Lv, C.; Chen, C.; Chuang, Y.-C.; Tseng, F.-G.; Yin, Y.; Grey, F.; Zheng, Q. Substrate curvature gradient drives rapid droplet motion. *Phys. Rev. Lett.* **2014**, *113*, No. 026101.

(4) Roy, A. C.; Yadav, M.; Arul, E. P.; Khanna, A.; Ghatak, A. Generation of aspherical optical lenses via arrested spreading and pinching of a cross-linkable liquid. *Langmuir* **2016**, *32*, 5356−5364.

(5) Kadhim, M. A.; Kapur, N.; Summers, J. L.; Thompson, H. Experimental and theoretical investigation of droplet evaporation on heated hydrophilic and hydrophobic surfaces. *Langmuir* **2019**, *35*, 6256−6266.

(6) Shen, Y.; Cheng, Y. P.; Xu, J. L.; Zhang, K.; Sui, Y. Theoretical analysis of a sessile evaporating droplet on a curved substrate with an interfacial cooling effect. *Langmuir* **2020**, *36*, 5618−5625.

(7) Lafuma, A.; Quéré, D. Superhydrophobic states. *Nat. Mater.* **2003**, *2*, 457.

(8) Zheng, Q. S.; Yu, Y.; Zhao, Z. H. Effects of hydraulic pressure on the stability and transition of wetting modes of superhydrophobic surfaces. *Langmuir* **2005**, *21*, 12207−12212.

(9) Li, H.; Yan, T.; Fichthorn, K. A.; Yu, S. Dynamic contact angles and mechanisms of motion of water droplets moving on nanopillared superhydrophobic surfaces: a molecular dynamics simulation study. *Langmuir* **2018**, *34*, 9917−9926.

(10) Barthlott, W.; Neinhuis, C. Purity of the sacred lotus, or escape from contamination in biological surfaces. *Planta* **1997**, *202*, 1−8.

(11) Feng, L.; Li, S.; Li, Y.; Li, H.; Zhang, L.; Zhai, J.; Song, Y.; Liu, B.; Jiang, L.; Zhu, D. Super-hydrophobic surfaces: from natural to artificial. *Adv. Mater.* **2002**, *14*, 1857−1860.

(12) Ng, T. W.; Yu, Y.; Tan, H. Y.; Neild, A. Capillary well microplate. *Appl. Phys. Lett.* **2008**, *93*, 174105.

(13) Yu, Y.; Wang, X.; Ng, T. W. Modeling the liquid filling in capillary well microplates for analyte preconcentration. *J. Colloid Interface Sci.* **2012**, *376*, 269−273.

(14) Gurera, D.; Bhushan, B. Designing bioinspired conical surfaces for water collection from condensation. *J. Colloid Interface Sci.* **2020**, *560*, 138−148.

(15) Huang, G.; Li, M.; Yang, Q.; Li, Y.; Liu, H.; Yang, H.; Xu, F. Magnetically actuated droplet manipulation and its potential biomedical applications. *ACS Appl. Mater. Interfaces* **2017**, *9*, 1155−1166.

(16) Young, T. III. An essay on the cohesion of fluids. *Philos. Trans. R. Soc. London* **1805**, *95*, 65−87.

(17) Orr, F. M.; Scriven, L. E.; Rivas, A. P. Pendular rings between solids: meniscus properties and capillary force. *J. Fluid Mech.* **1975**, *67*, 723−742.

(18) Landau, L. D.; Lifshitz, E. M. *Fluid Mechanics*; 2nd ed., Pergamon Press: Oxford, 1987; 242−243.

(19) Extrand, C. W.; Moon, S. I. Contact angles of liquid drops on super hydrophobic surfaces: Understanding the role of flattening of drops by gravity. *Langmuir* **2010**, *26*, 17090−17099.

(20) Srinivasan, S.; McKinley, G. H.; Cohen, R. E. Assessing the accuracy of contact angle measurements for sessile drops on liquid-repellent surfaces. *Langmuir* **2011**, *27*, 13582−13589.

(21) Park, J.; Park, J.; Lim, H.; Kim, H.-Y. Shape of a large drop on a rough hydrophobic surface. *Phys. Fluids* **2013**, *25*, No. 022102.
(22) Lu, Z.; Ng, T. W.; Yu, Y. Fast modeling of clam-shell drop morphologies on cylindrical surfaces. *Int. J. Heat Mass Transfer* **2016**, *93*, 1132−1136.
(23) Raj, R.; Adera, S.; Enright, R.; Wang, E. N. High-resolution liquid patterns via three-dimensional droplet shape control. *Nat. Commun.* **2014**, *5*, 4975.
(24) Kumar, A.; Raj, R. Droplets on microdecorated surfaces: evolution of the polygonal contact line. *Langmuir* **2017**, *33*, 4854−4862.
(25) Li, H.; Yan, T.; Fichthorn, K. A. Influence of gravity on the sliding angle of water drops on nanopillared superhydrophobic surfaces. *Langmuir* **2020**, *36*, 9916−9925.
(26) McHale, G.; Newton, M. I. Liquid marbles: topical context within soft matter and recent progress. *Soft Matter* **2015**, *11*, 2530−2546.
(27) Li, J.; Zhou, X.; Li, J.; Che, L.; Yao, J.; McHale, G.; Chaudhury, M. K.; Wang, Z. Topological liquid diode. *Sci. Adv.* **2017**, *3*, eaao3530.
(28) Ren, H.; Wu, S.-T. Variable-focus liquid lens by changing aperture. *Appl. Phys. Lett.* **2005**, *86*, 211107.
(29) Mishra, K.; van den Ende, D.; Mugele, F. Recent developments in optofluidic lens technology. *Micromachines* **2016**, *7*, 102.
(30) Whyman, G.; Bormashenko, E. Oblate spheroid model for calculation of the shape and contact angles of heavy droplets. *J. Colloid Interface Sci.* **2009**, *331*, 174−177.
(31) Lubarda, V. A.; Talke, K. A. Analysis of the equilibrium droplet shape based on an ellipsoidal droplet model. *Langmuir* **2011**, *27*, 10705−10713.
(32) Wang, X.; Yu, Y. Analysis of the shape of heavy droplets on flat and spherical surface. *Sci. China Phys. Mech. Astron.* **2012**, *55*, 1118−1124.
(33) Erbil, H. Y.; Meric, R. A. Evaporation of sessile drops on polymer surfaces: Ellipsoidal cap geometry. *J. Phys. Chem. B* **1997**, *101*, 6867−6873.
(34) Wang, Z. L.; Chen, E. H.; Zhao, Y. P. The effect of surface anisotropy on contact angles and the characterization of elliptical cap droplets. *Sci. China-Technol. Sci.* **2018**, *61*, 309−316.
(35) Vakarelski, I. U.; Patankar, N. A.; Marston, J. O.; Chan, D. Y. C.; Thoroddsen, S. T. Stabilization of Leidenfrost vapour layer by textured superhydrophobic surfaces. *Nature* **2012**, *489*, 274−277.
(36) Dupeux, G.; Bourrianne, P.; Magdelaine, Q.; Clanet, C.; Quéré, D. Propulsion on a superhydrophobic ratchet. *Sci. Rep.* **2014**, *4*, 5280.

https://dx.doi.org/10.1021/acsomega.0c03700
ACS Omega 2020, 5, 26732−26737